Fluorescence Depolarization of Actin Filaments in Reconstructed Myofibers: The Effect of S1 or pPDM-S1 on Movements of Distinct Areas of Actin

Yu. S. Borovikov,* I. V. Dedova,† C. G. dos Remedios,† N. N. Vikhoreva,* P. G. Vikhorev,* S. V. Avrova,* T. L. Hazlett,‡ and B. W. Van Der Meer§

*Institute of Cytology, Russian Academy of Science, St. Petersburg 194064, Russia; †Institute for Biomedical Research, University of Sydney, Sydney NSW 2006, Australia; ‡Laboratory for Fluorescence Dynamics, University of Illinois at Urbana-Champaign, Urbana, Illinois 61801-3080 USA; and §Department of Physics and Astronomy, Western Kentucky University, Bowling Green, Kentucky 42101-3576 USA

ABSTRACT Fluorescence polarization measurements were used to study changes in the orientation and order of different sites on actin monomers within muscle thin filaments during weak or strong binding states with myosin subfragment-1. Ghost muscle fibers were supplemented with actin monomers specifically labeled with different fluorescent probes at Cys-10, Gln-41, Lys-61, Lys-373, Cys-374, and the nucleotide binding site. We also used fluorescent phalloidin as a probe near the filament axis. Changes in the orientation of the fluorophores depend not only on the state of acto-myosin binding but also on the location of the fluorescent probes. We observed changes in polarization (i.e., orientation) for those fluorophores attached at the sites directly involved in myosin binding (and located at high radii from the filament axis) that were contrary to the fluorophores located at the sites close to the axis of thin filament. These altered probe orientations suggest that myosin binding alters the conformation of F-actin. Strong binding by myosin heads produces changes in probe orientation that are opposite to those observed during weak binding.

INTRODUCTION

Muscle contraction is generated by the interaction of myosin cross-bridges with actin filaments and ATP. During force generation, the myosin cross-bridges cycle through several conformational states, the most significant of which are the so-called ''strong'' and ''weak'' forms of myosin binding to actin (Lymn and Taylor, 1971).

The strong binding states of myosin for actin (nucleotide-free actomyosin (AM) and actomyosin-ADP (AM-ADP)) are characterized by a high affinity for actin, slow kinetics of myosin attachment/detachment from actin filaments, and the capacity of regulated actin to cooperatively activate myosin (Bremel and Weber, 1972; White and Taylor, 1976). On the other hand, the weak binding states (AM-ATP and AM-ADP-Pi) are characterized by a low actomyosin affinity, fast kinetics, and no thin filament cooperativity (Lymn and Taylor, 1971; Chalovich et al., 1983).

It is widely accepted that myosin cross-bridges undergo structural changes during the force-generation process (Cooke, 1997). Current models involve large-scale rotation of the light chain domain relative to the actin-binding/catalytic domain, which itself does not rotate during contraction (dos Remedios et al., 1972; Rayment et al., 1993). The large free-energy change upon binding of the myosin head to actin may also be able to generate conformational change in actin (Geeves, 1991).

X-ray studies on muscle fibers (Kojima et al., 1994) and on intact muscle (Huxley et al., 1994; Wakabayashi et al., 1994) have suggested that extensibility of the actin filament provides nearly half of the sarcomere compliance of an active muscle during isometric contraction. Wakabayashi et al. (1994) also observed that during isometric contraction, there are changes in the helical structure of F-actin including variations in the axial rise per monomer, and variations in the genetic and long pitch helices (Wakabayashi et al., 1994). Egelman et al. (1982) and Stokes and DeRosier (1987) emphasized the existence of variations in the twist along the axes of isolated filaments, which increases the fluctuations of the azimuthal angle between adjacent monomers by ~10°. Some regions of actin appear to shift when myosin binds (Popp et al., 1991). Others have also suggested that such conformational changes are cooperative (Orlova and Egelman, 1997).

Numerous spectroscopic studies have indicated that contraction depends on local as well as global structure and dynamics of F-actin in the nanosecond-millisecond range (Kouyama and Mihashi, 1980; Yanagida et al., 1984). Myosin increases bending flexibility of thin filaments (Yanagida et al., 1984), and decreases the internal motions in actin (Prochniewicz and Thomas, 1997). Polarization fluorimetry is highly sensitive to conformational changes in F-actin (Borovikov and Kakol, 1991), myosin (dos Remedios et al., 1972; Borovikov and Levitsky, 1989; Burghardt et al., 2001), and tropomyosin (Szczesna et al., 1989).

In this report we study movements of different polypeptide chains within F-actin monomers during strong and

Submitted August 23, 2003, and accepted for publication January 9, 2004.

Address reprint requests to Cristobal G. dos Remedios, Muscle Research Unit, Rm. 10, Institute for Biomedical Research, University of Sydney, Sydney NSW 2006, Australia. Tel.: 61-2-93513209; E-mail: crisdos@anatomy.usyd.edu.au.

0006-3495/04/05/3020/10 $2.00

weak binding with myosin. We use nine fluorescent probes attached at five loci as well as labeled phalloidin and ε-ADP to detect orientation changes that reflect movement of the actin (Yanagida and Oosawa, 1978; Borovikov, 1999).

MATERIALS AND METHODS

Chemicals were obtained from Sigma (St. Louis, MO). Iodoacetamide 5-fluorescein (5-IAF), dansyl ethylenediamine (DED), and fluorescein-maleimide were purchased from Molecular Probes (Eugene, OR); adenosine 5′-triphosphate (ATP) and β-mercaptoethanol were from Merck (Darmstadt, Germany); the Bradford protein assay reagent was purchased from BioRad (Munich, Germany), and NaN_3 was from Fluka (Buchs, Switzerland).

Actin was isolated from acetone powder prepared from the white leg and back muscles of adult rabbits (Spudich and Watt, 1971) and was stored as F-actin with continuous dialysis against F-buffer (10 mM MOPS, 100 mM KCl, 2 mM $MgCl_2$, 0.2 mM $CaCl_2$, 1 mM NaN_3, 0.2 mM ATP, pH 7.0) at 4°C.

Rabbit skeletal muscle myosin subfragment-1 (S1) was prepared by α-chymotrypsin digestion of myosin in 0.12 M KCl, 2 mM EGTA, and 20 mM Tris/HCl, pH 6.8 for 10 min at 25°C (Weeds and Pope, 1977). S1 was reacted with pPDM (*N,N′*-p-phenylenedimaleimide) (pPDM-S1) at 0°C (Wells and Yount, 1979) and further purified with F-actin. pPDM-S1 and S1 were used as models of the weak- and the strong-binding states, respectively (Chalovich et al., 1983; Borovikov and Kakol, 1991).

Protein concentration was determined by the method of Lowry et al. (1951) or spectrophotometrically using 0.63 mg ml^{-1} cm^{-1} at 290 nm and 42,000 for actin, and 0.75 mg ml^{-1} cm^{-1} at 280 nm and 110,000 for S1. The proteins were assayed for purity using SDS-PAGE gel electrophoresis. Actin was labeled at Cys-374 with 1,5-IAEDANS or fluorescein-maleimide as described earlier (Miki et al., 1987). The labeling ratio for 1,5-IAEDANS (0.8–0.9, $n = 5$) was calculated using an absorption coefficient of 6,100 M^{-1} cm^{-1} at 336 nm (Hudson and Weber, 1973). The labeling ratio for fluorescein-maleimide was 0.5–0.6 ($n = 4$).

Labeling of Cys-374 with 5-IAF was performed as described by Moens et al. (1994). The concentration of the label was calculated using an absorption coefficient of 77,000 M^{-1} cm^{-1} at 496 nm (Takashi, 1979). The average degree of labeling was 0.55 ($n = 6$). The DED probe was enzymatically bound to Gln-41 (Kim et al., 1996). Labeling ratios for six different preparations were between 0.63 and 0.9.

Labeling of Lys-61 with fluorescein isothiocyanate (FITC) was carried out according to Miki et al. (1987). The concentration of the FITC label in the sample was calculated using an absorption coefficient of 74,500 M^{-1} cm^{-1} at 493 nm. The mean labeling ratio was 0.8 for five preparations. Cys-10 was modified with fluorescein-maleimide, 1,5-IAEDANS, or 5-IAF as described elsewhere (Drewes and Faulstich, 1991). The labeling ratios were between 0.4 and 0.6 ($n = 7$). Labeling of Lys-373 with NBD-Cl (7-chloro-4-nitrobenzeno-2-oxa-1,3-diazole) was performed essentially as described elsewhere (Detmers et al., 1981). The specificity of labeling was confirmed from proteolytic fragments on SDS-PAGE gels.

Ghost fibers were prepared from single glycerinated rabbit skeletal muscle fibers by extraction of myosin and the regulatory proteins as described earlier (Borovikov and Gusev, 1983). The reconstruction of filaments from exogenous G-actin within the fibers was performed as described elsewhere (Borovikov et al., 2000). Ghost fibers were incubated for 20–30 min at 20°C in G-actin (2–4 mg/ml). Then 100 mM KCl, 1 mM $MgCl_2$, 20 mM Tris/HCl buffer, pH 7.5 were added to the bathing solution for 20–30 min to polymerize the G-actin.

Reconstructed ghost fibers generally contained ~50% of exogenous actin (Borovikov et al., 2000). The degree of incorporation (30–80%) had no effect on conformational changes in actin induced by S1 (Khoroshev and Borovikov, 1991). Electron microscope observation shows no difference between native thin filaments and those containing fluorescent actin (Khorochev et al., 2000). Besides, in fibers containing fluorescent actin, it is possible to reconstruct a troponin-tropomyosin system and incorporate myosin. These fibers are Ca^{2+}-sensitive and contract like the native fibers, indicating that fluorescent actin is incorporated normally into thin filaments and that there is no difference in myosin heads binding to modified and native actin. Labeling of F-actin in ghost fibers with tetramethylrhodamine isothiocyanate (TRITC)-phalloidin or FITC-phalloidin was performed by incubation of the fibers in 20 mM KCl, 1 mM $MgCl_2$, and 6.7 mM phosphate buffer, pH 7.0, with 40 μM phalloidin. To prevent the labeling of endogenous filaments, the ghost fibers were treated with 0.1 mM phalloidin for 1 h before the incorporation of exogenous G-actin. ε-ADP was incorporated into the F-actin of ghost fibers by the method of Yanagida and Oosawa (1978).

Either S1 or pPDM-S1 was incorporated into ghost fibers using 20 mM KCl, 3 mM $MgCl_2$, 1 mM DTT, 10 mM Tris/HCl, pH 6.8, and 2.0–2.5 mg/ml S1 or pPDM-S1 (Borovikov et al., 1996). The concentration of weakly bound pPDM-S1 in ghost fibers was optimized using 0.5–1.0 mg/ml pPDM-S1. Incorporation of S1 and pPDM-S1 were confirmed by SDS-PAGE electrophoresis (Laemmli, 1970) and the molar ratios of S1 or pPDM-S1 bound to the ghost fibers were determined densitometrically (UltroScan XL, Pharmacia, Uppsala, Sweden).

Fluorescence polarization of single ghost fibers was determined using a microspectrophotometer (Fig. 1) (Ioffer et al., 1974). The intensities of the four components of polarized fluorescence were measured parallel ($_{\parallel}I_{\parallel}$, $_{\parallel}I_{\perp}$) and perpendicular ($_{\perp}I_{\perp}$, $_{\perp}I_{\parallel}$) to the fiber axis relative to the polarization plane of the exiting light. Four fluorescence polarization ratios were defined as:

$$P_{\parallel} = ({}_{\parallel}I_{\parallel} - {}_{\parallel}I_{\perp})/({}_{\parallel}I_{\parallel} - {}_{\parallel}I_{\perp}),$$

$$P_{\perp} = ({}_{\perp}I_{\perp} - {}_{\perp}I_{\parallel})/({}_{\perp}I_{\perp} - {}_{\perp}I_{\parallel}),$$

$$Q_{\parallel} = ({}_{\parallel}I_{\parallel} - {}_{\perp}I_{\parallel})/({}_{\parallel}I_{\parallel} + {}_{\perp}I_{\parallel}),$$

$$Q_{\perp} = ({}_{\perp}I_{\perp} - {}_{\parallel}I_{\perp})/{}_{\perp}I_{\perp} + {}_{\parallel}I_{\perp}),$$

where $Q_{\perp}$ depends on the other three ratios:

$$Q_{\perp} = (P_{\perp} + P_{\parallel} - Q_{\parallel} - P_{\perp}P_{\parallel}Q_{\parallel})/ (1 + P_{\perp}P_{\parallel} - P_{\parallel}Q_{\perp} - P_{\perp}Q_{\parallel}).$$

The most significant systematic errors in measuring polarization of fluorescence are caused by the depolarization of exciting and emitted light arising from the dichroic mirror, the high numerical aperture of the objective (Borejdo et al., 1982), and photobleaching (Kishino and Yanagida, 1988). Since the objective aperture was 0.80, the depolarization of the exciting light is neglected (Borovikov et al., 1974). Photobleaching was minimal because the light intensity was low (typically 0.1 mW) and all solutions contained 0.1% β-mercaptoethanol. We corrected for the dichroic mirror using a solution of free fluorescent dyes where $_{\parallel}I_{\parallel} = {}_{\parallel}I_{\perp} = {}_{\perp}I_{\perp} = {}_{\perp}I_{\parallel}$. An instrumental correction was used to satisfy this condition. Nonspecific covalent probes can also cause marked fluorescence depolarization. Here, G-actin was modified specifically by fluorescent dyes before incorporation into ghost fiber filaments, which excludes the modification of other proteins (Borovikov et al., 2000).

The polarized fluorescence from ε-ADP was measured at 330–450 nm after excitation at 310 ± 5 nm; 1,5-IAEDANS-actin emission was recorded at 480–550 nm using 365 ± 5 nm excitation. Emissions from 5-IAF, NBD-Cl, FITC, DED, fluorescein-maleimide, TRITC-phalloidin, and FITC-

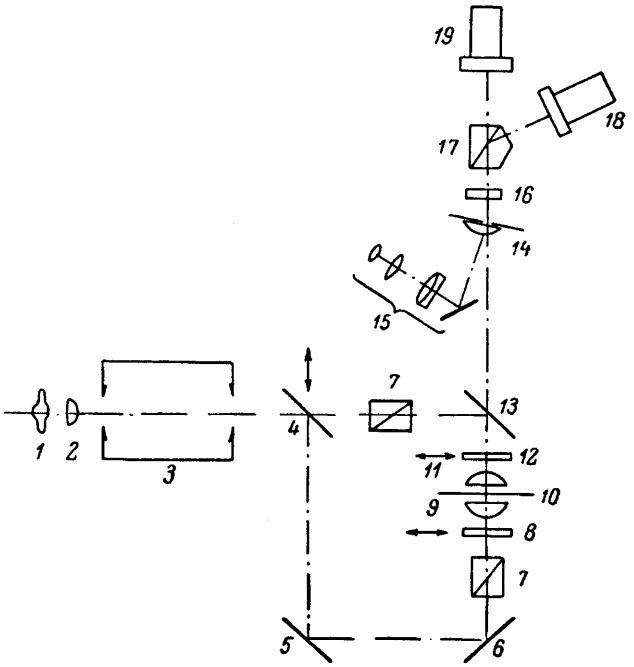

FIGURE 1 Microspectrophotometer design. A 250 W mercury lamp DRSH-250 (*1*) source passed through a quartz lens (*2*) and a double monochromator (*3*) and is split into two polarized beams by a polarizing prism (*7*). The ordinary polarized beam was reflected at the dichroic mirror (*13*) and was condensed by a quartz objective (UV 58/0.80) (*11*) on a fiber in the cell on the microscope stage (*10*). The emitted light from the fiber was collected by the objective (*11*) and led to a concave mirror with a small hole (*14*). After passing through lens and a barrier filter (*16*), the beam was separated by a Wollaston prism (*17*) into polarized beams perpendicular and parallel to the fiber axis. The intensities of the two beams were detected by two photomultiplier tubes (*18* and *19*).

phalloidin were recorded at 500–600 nm after excitation at 437 ± 5 nm. Fluorescence intensities were made at five positions along a fiber and before and after decorating actin filaments with S1 or pPDM-S1.

Analysis of the polarized fluorescence allows a determination of the arrangement and rotational mobility of the fluorophores in an average protein molecule. The fiber sample has cylindrical or azimuthal symmetry around the fiber axis resulting in four different parameters—S_A, S_E, C_P, and C_M—that completely determine the polarization ratios. S_A describes the alignment of the absorption dipoles with the fiber axis. In the hypothetical sample where all absorption dipoles align with the fiber axis, $S_A = 1$. If all dipoles are perpendicular to the axis, S_A is -0.5. $S_A = 0$ if these dipoles are completely random or if they all are at 54.7° from the fiber axis. If all dipoles have the same angle (Φ_A) with the fiber axis, S_A is $3/2 \cos^2 \Phi_A - 1/2$. Similarly, S_E describes the alignment between the emission dipoles and the fiber axis. Neither S_A nor S_E depend on the rate of motion or the average fluorescence lifetime, whereas C_P (the ''polar'' correlation) and C_M (the ''mixed'' correlation) do. In steady-state experiments, they depend on the ratio of the fast rotational correlation time over the average fluorescence lifetime. They also depend on the orientational order. In the hypothetical case that both the absorption dipoles and the emission dipoles have very sharp peaks and have essentially one angle with the fiber axis, $C_P = S_A \times S_E$. C_M is a time-average and distribution-average of a function of both polar and azimuthal angles of the absorption dipoles and of the emission dipoles.

There are two interesting approximations: the perfect-azimuthal-correlation (PAC) approximation and the zero-azimuthal-correlation (ZAC) approximation. In the first it is assumed that at all times any absorption dipole and the corresponding emission dipole move in a ''vertical'' plane where the absorption dipole, its emission dipole, and the fiber axis are always in the same plane. Here, the relation $C_M = 1/6(1 - S_A - S_E + C_P)$. Consequently, S_A, S_E, C_P, and C_M can be calculated from data for $P_\parallel$, $P_\perp$, and $Q_\parallel$ in this approximation. In the ZAC approximation, it is assumed that the azimuthal angle φ_{A0Et} is essentially random. This angle is defined as follows: imagine a plane perpendicular to the fiber axis; project all absorption dipoles and all emission dipoles on this plane. The angle φ_{A0Et} is the angle between the projection of the absorption dipole at the moment of absorption of the exciting photon and that of the emission dipole at the moment of emission of its photon. Here, $C_M = zero$, we can again calculate S_A, S_E, C_P, and C_M from data for $P_\parallel$, $P_\perp$, and $Q_\parallel$. Experimental data for $P_\parallel$, $P_\perp$, and $Q_\parallel$ have been analyzed in both approximations. Note that the two sets of results for S_A, S_E, C_P, and C_M represent two opposite limits, between which the ''true'' set is located.

We assume that the distribution of angles between the absorption dipole and the fiber axis has a relatively sharp peak at Φ_A and that the emission dipoles are distributed similarly around a peak at Φ_E. Estimates for these peak angles can be obtained from S_A and S_E using the following equations:

$$\Phi_A = \sin^{-1}\left(\sqrt{\frac{2}{3}(1 - S_A)}\right)$$

$$\Phi_E = \sin^{-1}\left(\sqrt{\frac{2}{3}(1 - S_E)}\right).$$

We have also utilized a model-dependent analysis to quantitatively assess changes in the probe orientation (Kaulin, 1968; Rozanov et al., 1971; Andreev et al., 1995; Irving et al., 1995). In particular, we have used the helix plus isotropic (H + I) model (Tregear and Mendelson, 1975; Borejdo and Putnam, 1977; Irving, 1996), which assumes there are two populations of probes on the fiber. One population is completely disordered (N), while the second, ($1 - N$), has absorption transition dipoles ($\vec{A}$) at a fixed angle Φ_A relative to the fiber axis with their emission transition dipoles ($\vec{E}$) at a fixed angle Φ_E from this axis.

Labeled G- or F-actin were mixed with a twofold excess of S1 and incubated at room temperature for 15–20 min to ensure complete hydrolysis of ATP remaining in the actin. The final concentration of actin was 1.5–3 μM. F-actin was stabilized against dilution-induced depolymerization by equimolar phalloidin. Control experiments confirmed that dilution of F-actin in the presence of up to 1.4 μM phalloidin did not decrease the sedimentation of F-actin. Fluorescence experiments did not require removal of oxygen, as fluorescence intensity remained at a constant for at least 30 min illumination by the exciting light.

Steady-state anisotropy measurements were performed using a PC1 spectrofluorometer (ISS, Champaign, IL). The fluorescence anisotropy of each sample was obtained at room temperature in G- or F-buffer with 92% glycerol. Anisotropy values were collected as the sample was cooled to −20°C. Limiting anisotropy values (r_0) were obtained by plotting the dependency of the anisotropy against the solvent temperature/viscosity and extrapolating to zero (Perrin plot). Typically, the extrapolated value was within 5% of the sample anisotropy at −20°C.

1,5-IAEDANS was excited at 365 ± 5 nm and recorded at 480−550 nm. The fluorescence from 5-IAF, NBD-Cl, FITC, DED, fluorescein-maleimide, TRITC-phalloidin, and FITC-phalloidin was excited at 487 ± 5 nm and recorded at 500−600 nm.

The angle between absorption and emission dipoles of a probe (γ) was calculated using

$$\gamma = \cos^{-1}\left(\sqrt{\frac{5}{3}r_0 + \frac{1}{3}}\right),$$

where r_0 is the limiting anisotropy. Fluorescence lifetime and anisotropy decay data were obtained on a homebuilt multi-frequency phase and modulation fluorimeter based on the Gratton design (Gratton and Limkeman, 1983). Excitation of the fluorescein and rhodamine derivatives was accomplished using the 488 nm and the 514 nm lines of a Spectra-Physics (Mountain View, CA) model 2017 argon ion laser. The laser output was then modulated using an electro-optic modulator (ISS). Dansyl and IAEDANS derivatives were excited using the pulsed 345 nm output of a frequency-double, cavity-dumped, DCM dye laser (Coherent, Palo Alto, CA,) pumped using a mode locked Nd:YAG laser (Coherent). The fluorescence was collected through optical filters to remove scattered excitation light. A long-pass Schott OG 515 glass filter (Schott Glass Technologies, Duryea, PA) removed the 488 nm scatter, a long-pass HOYA O-54 glass filter (HOYA, Singapore) eliminated the 514 nm scatter, and a long-pass Schott KV399 filter eliminated scatter from 345 nm excitation light. Polarization artifacts were eliminated in the intensity decay measurements by setting the excitation and emission polarizers to magic angle conditions. The excitation beam was polarized normal to the laboratory plane, 0°, and the emission was observed through a polarizer set to 54.7° (Spencer and Weber, 1970). Lifetime standards used for 488 nm, 514 nm, and 345 nm excitation wavelengths were fluorescein in 0.01 M NaOH (4.05 ns), rhodamine 6G in ethanol (3.89 ns), and POPOP in ethanol (1.35 ns), respectively. Intensity decay and anisotropy decay data were analyzed with multiexponential decay models using the Globals Unlimited software package (Laboratory for Fluorescence Dynamics, University of Illinois, Urbana, IL). Intensity decay data were well fit using a double exponential decay model. Time-resolved anisotropy data were analyzed assuming a single, fluorophore-labeled specie having two rotational correlation times, ϕ_1 and ϕ_2. Intensity and anisotropy data were fit using nonlinear least-squares procedures with the best fit judged by the reduced χ^2. Errors for the phase and modulation data were set to 0.2° and 0.004, respectively.

RESULTS

Fluorescence and anisotropy decays of G-actin and F-actin ± myosin S1

Fluorescence decays of probes in F-actin show a long-lived, major lifetime component (τ_1) that represents 80–98% of the decay fractional intensity (Table 1). The second lifetime component, τ_2 represents the remaining amplitude and is from ~4- to 5-fold shorter than τ_1. As can be seen from Table 1, binding of S1 does not change the lifetimes of fluorophores significantly. This suggests that S1 has a negligible effect on the environment of the probes. Two rotational correlation times, φ_1 and φ_2, are resolved for each probe. A large fraction of the anisotropy decay (45–85%) is derived from a relatively slow rotation where $\varphi_1/\langle\tau\rangle$ was 3.1 or higher. It is no less than a factor of 20 slower than the faster rotational component, φ_2. In many cases, $\varphi_1/\langle\tau\rangle$ is >10, i.e., conditions where the rate of the slow motion cannot be accurately determined due to the shortness of the average fluorescence lifetime. The fast rotational correlation time, $\varphi_2/\langle\tau\rangle$, between 0 and 0.4, represents a lesser, but still significant, decay (15–56%), indicating the presence of rapid motion at the fluorophore attachment sites (''wobble''). In addition, our results show that the presence of S1 has little or no effect on the fraction of the relatively slow rotational motion (Table 1). This result suggests S1 has little impact on the amplitude of the wobble and thus does not appreciably hinder the local flexibility at the probe attachment sites, at least in solution.

Table 2 summarizes the measured fluorescence anisotropy values for fluorophores in G- and F-actin obtained in solvents of two different viscosities, namely in buffer at 22°C (r_{ss}) and in 92% glycerol at −20°C (r_0). Anisotropies of dyes increased dramatically with an increase of the viscosity of the environment. The difference between the values of r_0 and r_{ss} suggests that dyes may be bound to the mobile polypeptide chains within the actin molecule and that these chains become restrained in the viscous solvent. Fluorescence anisotropy values of the labels attached to Cys-374 and Gln-41 increased upon polymerization. However, there was no polymerization-induced change in the r_{ss} values obtained for the FITC probe located at Lys-61 (Table 2). Binding of S1 significantly increases the anisotropy of 1,5-IAEDANS, DED, FITC, and TRITC-phalloidin (Table 2). However, there were only minor changes in anisotropy of 5-IAF due to S1 binding.

The r_0 values from the time-resolved measurements (Table 1) qualitatively agreed with those found from steady-state measurements at high viscosity (matched within 12%) (Table 2). Several values, however, deviated by greater amounts. The steady-state values are more robust and we consider them to be reliable, although 92% glycerol contributed to the observed disparities. More likely, these discrepancies are due to a decay that is more complex than the double exponential model used to derive the data. For all probes, the r_0 in Table 2 is greater than that in Table 1. This difference indicates there may be some fast motion that is not defined and represents an anisotropy decay outside the time resolution of the instrument used.

We calculated (Takashi et al., 1976) the angles between absorption and emission dipoles of the probes (γ) from r_0 values of Table 2. The angles between absorption and emission dipoles for most labels were below 24°. TRITC-phalloidin and 5-IAF had the smallest γ (14–16°). The value for 1,5-IAEDANS (24.1°) agrees well with previous results (Hudson and Weber, 1973). Binding of S1 resulted in moderate 1–2° alterations of the γ-values, which suggests that S1 does not significantly affect the relative orientation of the absorption and emission dipoles. The only exception was the FITC, for which the angle between absorption and emission dipoles increased by 8° in the presence of S1.

The parameter r_{ss}/r_0 is a measure for the overall degree of restriction in the motion of the fluorophore. A value near unity signifies complete restriction, whereas zero indicates the absence of hindrance to the motion. Binding of S1 resulted in an increase of r_{ss}/r_0 for all probes, suggesting that S1 binding restricts probe motion. However, the level of this increase varies widely: from 3% (5-IAF) to 83% (1,5-IAEDANS), both attached to Cys-374. Moreover, the modes of these restrictions also vary. For example, in Table 1 we see that for TRITC-phalloidin, close to the filament axis, S1 binding induces a decrease in φ_1 andφ_2 with a subsequent

TABLE 1 Lifetimes (τ_1 and τ_2) and rotational correlation times (φ_1 and φ_2) of the fluorescent probes attached to different sites on F-actin in the absence and presence of S1

Dye (labeling site)	Sample	τ_1 (ns)	Fraction for τ_1	τ_2 (ns)	$\langle\tau\rangle$ (ns)	χ^2	r_0	$\varphi_1/\langle\tau\rangle$	Fraction for φ_1	$\varphi_2/\langle\tau\rangle$
TRITC-phalloidin (near the filament axis)	F-actin	2.8	0.795	1.12	2.46	0.382	0.339	4072.3	0.64	0.40
	F-actin-S1	2.7	0.795	1.13	2.37	0.513	0.345	45.3	0.64	0.33
1,5-IAEDANS (Cys-374)	F-actin	20.3	0.971	5.98	19.9	1.746	0.263	19.4	0.85	0.37
	F-actin-S1	19.9	0.983	2.47	19.6	2.024	0.293	510.1	0.85	0
DED (Gln-41)	F-actin	16.4	0.713	5.92	13.3	0.467	0.380	749.0	0.67	0.03
	F-actin-S1	17.1	0.653	7.05	13.4	2.624	0.410	748.6	0.61	0
5-IAF (Cys-374)	F-actin	4.33	0.928	1.33	4.10	3.761	0.323	12.0	0.61	0.12
	F-actin-S1	4.28	0.934	1.20	4.07	2.512	0.359	7.3	0.49	0.07
FITC (Lys-61)	F-actin	3.82	0.885	0.94	3.58	2.128	0.291	3.8	0.45	0.11
	F-actin-S1	3.83	0.873	1.07	3.46	0.735	0.270	5.6	0.46	0.16

$\langle\tau\rangle$ represents the intensity-weighted average of the two lifetimes, and χ^2 is the local χ-square value. r_0 is the initial time-resolved anisotropy.

decrease in the apparent r_0, whereas for FITC at Lys-61, S1 binding triggers changes in the rotational correlation times, but in the opposite direction.

Polarization ratios of labeled F-actin in ghost fibers

A summary of the fluorescence polarization ratios obtained from measurements on ghost fibers is shown in Table 3. The values $P_\parallel$ and $Q_\parallel$ are significantly greater than $P_\perp$ and $Q_\perp$ for 1,5-IAEDANS, 5-IAF, and fluorescein-maleimide attached at Cys-374, 1,5-IAEDANS at the Cys-10 residue, FITC at Lys-61, and finally, TRITC-phalloidin and FITC-phalloidin. Phalloidin binds close to the center of the filament in the groove between three neighboring actin monomers (Lorenz et al., 1993). Our data suggest that dipoles of these probes are preferentially oriented parallel to the fiber axis (Kakol et al., 1987). On the other hand, labels such as DED (attached to Gln-41) and ε-ADP (at the nucleotide binding site) had values $P_\perp$ and $Q_\perp$ greater than $P_\parallel$ and $Q_\parallel$. This suggests that the dipoles of these probes are preferentially oriented perpendicular to the fiber axis (Yanagida and Oosawa, 1978; Kakol et al., 1987). Although the values $P_\perp$ and $P_\parallel$ as well as $Q_\parallel$ and $Q_\perp$ for the labels attached to the Cys-374 residue differ significantly from each other, this difference was less pronounced for probes at the Cys-10 residue. This discrepancy may represent a higher degree of orientational order of the Cys-374 residues within a filament compared to the Cys-10 residues. This is consistent with the structure at these locations.

The fluorescence polarization data were analyzed using the PAC and ZAC approximations, and the H + I model

TABLE 2 Summary of steady-state anisotropy parameters obtained for different probes at specified locations on G- or F-actin in the presence and absence of S1

Dye (labeling site)	Sample	r_{ss}	r_0	r_{ss}/r_0	γ
TRITC-phalloidin near the filament axis	F-actin	0.174 ± 0.013	0.363 ± 0.003	0.479	14.4
	F-actin-S1	0.237 ± 0.011	0.349 ± 0.004	0.679	17.0
1,5-IAEDANS (Cys-374)	G-actin	0.120 ± 0.005	0.305 ± 0.001	0.393	23.4
	G-actin-S1	0.172 ± 0.001	0.300 ± 0.001	0.573	24.1
	F-actin	0.133 ± 0.010	0.300 ± 0.005	0.443	24.1
	F-actin-S1	0.240 ± 0.008	0.296 ± 0.002	0.811	24.6
DED (Gln-41)	G-actin	0.133 ± 0.003	0.335 ± 0.003	0.397	19.2
	G-actin-S1	0.256 ± 0.005	0.343 ± 0.004	0.746	18.0
	F-actin	0.226 ± 0.012	0.338 ± 0.001	0.669	18.8
	F-actin-S1	0.261 ± 0.005	0.343 ± 0.005	0.761	18.0
5-IAF (Cys-374)	G-actin	0.154 ± 0.002	0.354 ± 0.006	0.435	16.1
	G-actin-S1	0.155 ± 0.002	0.344 ± 0.003	0.451	17.8
	F-actin	0.165 ± 0.005	0.352 ± 0.003	0.469	16.4
	F-actin-S1	0.170 ± 0.007	0.351 ± 0.005	0.484	16.6
FITC (Lys-61)	G-actin	0.132 ± 0.002	0.358 ± 0.005	0.369	15.3
	G-actin-S1	0.141 ± 0.003	0.335 ± 0.003	0.421	19.2
	F-actin	0.133 ± 0.005	0.334 ± 0.005	0.398	19.4
	F-actin-S1	0.147 ± 0.001	0.274 ± 0.001	0.536	27.3

Fluorescence anisotropy was measured for the samples in G-buffer or F-buffer at 22°C (r_{ss}) and after samples were mixed with glycerol (92% final glycerol concentration) and cooled to −20°C (r_0). γ is the angle (in degrees) between the absorption and emission transition dipoles of the probe, and is calculated from r_0 (see Materials and Methods).

TABLE 3 Steady-state polarization ratios for ghost fibers in the presence and absence of S1 or pPDM-S1

Dye (labeling site)	Sample	N	$P_\parallel$	$P_\perp$	$Q_\parallel$	$Q_\perp$
FITC-phalloidin (near the filament axis)	F-A	12	0.394 ± 0.002	0.085 ± 0.002	0.420 ± 0.002	0.054 ± 0.002
	F-A-S1	12	0.398 ± 0.001	0.093 ± 0.002	0.436 ± 0.003	0.048 ± 0.002
TRITC-phalloidin (near the filament axis)	F-A	15	0.268 ± 0.002	−0.008 ± 0.003	0.156 ± 0.009	0.108 ± 0.008
	F-A-S1	15	0.314 ± 0.001	0.012 ± 0.002	0.204 ± 0.012	0.127 ± 0.012
	F-A-pPDM-S1	11	0.236 ± 0.003	0.022 ± 0.006	0.149 ± 0.015	0.112 ± 0.016
ε–ADP (between two domains)	F-A	8	−0.222 ± 0.005	0.529 ± 0.005	−0.610 ± 0.007	0.790 ± 0.005
	F-A-S1	8	−0.182 ± 0.009	0.510 ± 0.004	−0.539 ± 0.009	0.753 ± 0.007
1,5-IAEDANS (Cys-374)	F-A	12	0.303 ± 0.002	0.173 ± 0.003	0.347 ± 0.004	0.124 ± 0.004
	F-A-S1	6	0.216 ± 0.009	0.250 ± 0.004	0.235 ± 0.015	0.225 ± 0.010
	FA-pPDM-S1	6	0.299 ± 0.004	0.120 ± 0.014	0.395 ± 0.008	0.011 ± 0.004
1,5-IAEDANS (Cys-10)	F-A	18	0.243 ± 0.016	0.192 ± 0.006	0.336 ± 0.016	0.092 ± 0.026
	F-A-S1	8	0.224 ± 0.007	0.225 ± 0.004	0.255 ± 0.018	0.193 ± 0.015
	F-A-pPDM-S1	10	0.240 ± 0.007	0.149 ± 0.003	0.323 ± 0.008	0.061 ± 0.004
FM (Cys-374)	F-A	9	0.416 ± 0.012	0.179 ± 0.014	0.549 ± 0.017	0.005 ± 0.030
	F-A-S1	9	0.327 ± 0.016	0.303 ± 0.005	0.382 ± 0.044	0.237 ± 0.036
FM (Cys-10)	F-A	10	0.197 ± 0.003	0.189 ± 0.002	0.250 ± 0.005	0.135 ± 0.006
	F-A-S1	8	0.168 ± 0.001	0.170 ± 0.002	0.173 ± 0.002	0.166 ± 0.002
NBD-Cl (Lys-373)	F-A	12	0.294 ± 0.013	0.275 ± 0.012	0.313 ± 0.015	0.254 ± 0.030
	F-A-S1	11	0.064 ± 0.021	0.410 ± 0.007	0.044 ± 0.025	0.428 ± 0.007
5-IAF (Cys-374)	F-A	6	0.424 ± 0.003	0.191 ± 0.004	0.410 ± 0.009	0.207 ± 0.011
	F-A-S1	6	0.270 ± 0.003	0.264 ± 0.002	0.277 ± 0.009	0.254 ± 0.008
5-IAF (Cys-10)	F-A	8	0.210 ± 0.001	0.204 ± 0.002	0.233 ± 0.002	0.181 ± 0.004
	F-A-S1	6	0.212 ± 0.001	0.216 ± 0.001	0.235 ± 0.001	0.192 ± 0.003
DED (Gln-41)	F-A	15	0.274 ± 0.003	0.316 ± 0.002	0.257 ± 0.006	0.327 ± 0.007
	F-A-S1	13	0.225 ± 0.008	0.391 ± 0.005	0.219 ± 0.009	0.390 ± 0.011
FITC (Lys-61)	F-A	6	0.374 ± 0.006	0.127 ± 0.003	0.409 ± 0.007	0.086 ± 0.003
	F-A-S1	6	0.311 ± 0.006	0.155 ± 0.004	0.375 ± 0.012	0.081 ± 0.012

FM refers to fluorescein-maleimide. In the Sample column, F-actin is abbreviated to F-A. Polarization ratios, $P_\parallel$, $P_\perp$, $Q_\parallel$, and $Q_\parallel$ were fitted from an average of the ratios of ${}_\parallel I_\perp/{}_\parallel I_\parallel$, ${}_\perp I_\parallel/{}_\parallel I_\parallel$, and ${}_\perp I_\perp/{}_\parallel I_\perp$ (see Materials and Methods) and given as mean ± SE. n is the number of fibers used for measurements. The molar ratio of S1 or pPDM-S1 bound to actin in the fibers was 1:4.

(Kaulin, 1968; Rozanov et al., 1971; Tregear and Mendelson, 1975; Borejdo and Putnam, 1977; Wilson and Mendelson, 1983; Morales, 1984; Andreev et al., 1995; Irving, 1996). The results are summarized in Tables 4 and 5. In Table 5, the uncertainties in the angles are given for the H + I model. Uncertainties in the angles for the PAC approximations are similar.

Effect of S1 binding on fluorescence polarization ratios

Two groups of labeled sites respond to binding of S1 in opposite ways. The first consists of the phalloidin and ε-ADP sites. The second comprises Cys-10, Gln-41, Lys-61, Lys-373, and Cys-374. For the first group, binding of S1 to actin filaments in ghost fibers resulted in an increase in $P_\parallel$ and $Q_\parallel$, a decrease in $P_\perp$ and/or $Q_\perp$ (Table 3), an increase in S_A and S_E (Table 4), and a decrease in Φ_A and Φ_E (Table 5). In sum, a rotation of the labels toward the fiber axis is observed. For the second group, S1 binding triggered a decrease in $P_\parallel$ and $Q_\parallel$, and an increase in $P_\perp$ and/or $Q_\perp$ (Table 3), a decrease in S_A and S_E (Table 4), and an increase in Φ_A and Φ_E (Table 5). These labels appear to rotate away from the fiber axis. For FITC-phalloidin in the first group, the change in Φ_E was slight although the decrease in Φ_A and the increases in $P_\parallel$, $Q_\parallel$, S_A, and S_E were significant. In the second group, 5-IAF at Cys-10 produced changes in $P_\parallel$, $Q_\parallel$, and Φ_E that were not significant, although there were clear decreases in S_A and S_E, and the increases in $P_\perp$, $Q_\perp$, and Φ_A.

Saturation of changes in the angles Φ_A and Φ_E occurred at S1/actin ratios of 1:14. Further increases of this ratio resulted in a marked increase in the change of the angles Φ_A and Φ_E. Maximum changes in those polarization parameters were observed when the S1/actin ratio was 1:7. Further increases in S1 concentration caused no additional changes in Φ_A and Φ_E, suggesting that S1-induced changes in the polarization properties appear to have a cooperative nature.

We have used two different methods to analyze the fluorescence polarization data in the ghost fibers: a model-dependent method (the H + I model), and model-independent methods (PAC and ZAC, based on two opposite approximations). Both lead us to the same conclusion: namely that the angles for dyes at the periphery of the filament have opposite effects to those at its center when S1 binds. Furthermore, these changes have a cooperative nature and can be propagated along the actin filament.

TABLE 4 Values for S_A, S_E, C_P and C_M obtained from the data in Table 3 in the perfect-azimuthal-correlation approximation (PAC), in the zero-azimuthal-correlation (ZAC) approximation, and for the helix-isotropic model (H + I)

Sample/dye/site	S_A PAC	S_A H + I	S_A ZAC	S_E PAC	S_E H + I	S_E ZAC	C_P PAC	C_P H + I	C_P ZAC	C_M PAC	C_M H + I	C_M ZAC
F/Fp/axis	0.205	0.185	0.106	0.185	0.166	0.089	0.121	0.125	0.139	0.122	0.210	0
S/Fp/axis	0.214	0.198	0.115	0.185	0.170	0.090	0.126	0.132	0.143	0.121	0.202	0
F/Tp/axis	0.084	0.060	−0.002	0.167	0.140	0.069	0.031	0.044	0.063	0.130	0.326	0
S/Tp/axis	0.093	0.076	0.005	0.173	0.153	0.073	0.052	0.060	0.081	0.131	0.286	0
P/Tp/axis	0.080	0.054	−0.008	0.144	0.115	0.046	0.027	0.039	0.061	0.134	0.331	0
F/ε-A/b2d	−0.371	−0.393	−0.406	−0.212	−0.253	−0.290	0.088	0.112	0.132	0.278	0.693	0
S/ε-A/b2d	−0.346	−0.368	−0.387	−0.197	−0.238	−0.277	0.081	0.104	0.126	0.271	0.662	0
F/IA/Cys-374	0.137	0.109	0.036	0.106	0.078	0.010	0.090	0.097	0.115	0.141	0.200	0
S/IA/Cys-374	0.047	0.028	−0.052	0.035	0.012	−0.061	0.068	0.077	0.100	0.164	0.260	0
P/IA/Cys-374	0.206	0.158	0.105	0.134	0.092	0.043	0.089	0.118	0.112	0.125	0.168	0
F/IA/Cys-10	0.144	0.100	0.041	0.079	0.040	−0.013	0.074	0.104	0.102	0.142	0.194	0
S/IA/Cys-10	0.071	0.024	−0.028	0.051	0.008	−0.045	0.067	0.098	0.099	0.158	0.226	0
P/IA/Cys-10	0.156	0.109	0.055	0.096	0.054	0.005	0.066	0.113	0.094	0.136	0.239	0
F/FM/Cys-374	0.277	0.237	0.171	0.174	0.139	0.082	0.163	0.168	0.175	0.119	0.099	0
S/FM/Cys-374	0.088	0.084	0.017	0.053	0.030	0.046	0.117	0.119	0.141	0.163	0.121	0
F/FM/Cys-10	0.097	0.058	0.002	0.061	0.019	0.033	0.054	0.073	0.086	0.149	0.194	0
S/FM/Cys-10	0.061	0.011	0.034	0.057	0.008	0.037	0.038	0.059	0.074	0.153	0.241	0
F/NB/Lys-373	0.061	0.046	0.040	0.049	0.037	0.050	0.097	0.088	0.125	0.165	0.263	0
S/NB/Lys-373	0.103	0.122	0.190	0.093	0.112	0.182	0.064	0.073	0.104	0.210	0.474	0
F/5I/Cys-374	0.133	0.119	0.031	0.142	0.129	0.039	0.137	0.139	0.155	0.144	0.195	0
S/5I/Cys-374	0.049	0.037	0.050	0.044	0.031	0.054	0.086	0.089	0.116	0.166	0.287	0
F/5I/Cys-10	0.071	0.031	0.027	0.056	0.017	0.040	0.058	0.093	0.091	0.155	0.289	0
S/5I/Cys-10	0.066	0.028	0.033	0.050	0.014	0.045	0.061	0.096	0.094	0.157	0.286	0
F/DE/Gln-41	0.005	0.027	0.092	0.015	0.008	0.084	0.094	0.100	0.124	0.179	0.293	0
S/DE/Gln-41	0.044	0.118	0.139	0.041	0.038	0.136	0.094	0.109	0.127	0.196	0.376	0
F/FI/Lys-61	0.184	0.163	0.083	0.158	0.138	0.061	0.116	0.120	0.136	0.129	0.195	0
S/FI/Lys-61	0.166	0.133	0.065	0.120	0.089	0.026	0.094	0.103	0.118	0.135	0.168	0

The first column combines the information from the first two columns of Table 3. Abbreviations used: F, F-actin; S, F-actin-S1; P, F-actin-pPDM-S1; Fp, FITC-phalloidin; Tp, TRITC-phalloidin; εA, ε-ADP; IA, IAEDANS; FM, fluorescein maleimide; NB, NBD-Cl; 5I, 5-IAF; DE, DED; and FI, FITC. Axis stands for close-to-the-filament axis, and b2d for between two domains.
In the PAC and ZAC approximations, the parameters were calculated from the data in Table 3. For the H + I model, the parameters were calculated from the third, sixth, and eighth column of Table 5 using the γ-values indicated in Table 5.

The parameters C_P and C_M do not exhibit a clear trend with respect to either the location of the probes or the effects of S1 binding. Although the fraction N of disordered probes only refers to the H + I model and has no equivalent in the PAC and ZAC approximations, it is of interest to consider this parameter. Values of N for most of the dyes are <0.6 (Table 5), suggesting a high degree of order in the orientation of dye dipoles within a thin filament. The smallest values of N (0.06–0.4) were obtained for the ε-ADP phalloidin probes, located within the central areas of the actin filament. N-values were significantly higher for the following labels: 1,5-IAEDANS, fluorescein-maleimide, 5-IAF, NBD-Cl, DED, and FITC. These probes were attached to areas of actin monomers located on the periphery of the actin filament. Different numbers of randomly oriented probes obtained for the dyes located in the central and peripheral areas of the actin filament suggest different degrees in the order of the organization of these sites. The highest order is observed in the grooves between the long-pitch helices and the nucleotide binding site. The peripheral areas (Gln-41, Lys-61, Lys-373, and Cys-374) are less well ordered.

DISCUSSION

Time-resolved measurements have shown that dyes attached at specific sites in F-actin or in F-acto-S1 complexes had a large fraction with a rotational correlation time, φ_1, much larger than the average fluorescence lifetime, $\langle\tau\rangle$. A significant fraction had rotational correlation times, φ_2, much smaller than the average lifetime (Table 1). This suggests that protein reorientation (presumably described by φ_1) is relatively slow and that the probes exhibit fast random fluctuations (''wobble'', described by φ_2) around a well-defined orientation. However, our time-resolved data do not allow us to assume that the ratios $\langle\tau\rangle/\varphi_1$ and $\varphi_2/\langle\tau\rangle$ are essentially equal to zero for all probes.

To analyze the single-fiber polarization data, we initially employed an analysis model proposed by Dale et al. (1999). This method extracts detailed information on the orientation of the fluorophores and protein domains relative to the fiber axis. However, the model inherently assumes that $\langle\tau\rangle/\varphi_1$ and $\varphi_2/\langle\tau\rangle$ are close to zero, i.e., the rotational correlation time for protein reorientation is extremely large compared to the fluorescence lifetimes, and that the wobble is exception-

TABLE 5 The angles between the absorption dipoles and the fiber axis, Φ_A, those between the emission dipoles and the fiber axis, Φ_E for the PAC and ZAC approximations, and for the H + I model

Sample/dye/site	Φ_A PAC	Φ_A H + I	Φ_A ZAC	Φ_E PAC	Φ_E H + I	Φ_E ZAC	N H + I
F/Fp/axis	46.7	42.7 ± 0.2	50.5	47.5	43.9 ± 0.1	51.1	0.405 ± 0.003
S/Fp/axis	46.4	41.7 ± 0.2	50.2	47.5	43.5 ± 0.1	51.1	0.412 ± 0.003
F/Tp/axis	51.4	51.8 ± 0.2	54.8	48.2	48.0 ± 0.1	52.0	0.185 ± 0.008
S/Tp/axis	51.0	50.7 ± 0.3	54.5	47.9	46.7 ± 0.1	51.8	0.255 ± 0.003
P/Tp/axis	51.5	52.1 ± 0.2	55.0	49.1	49.2 ± 0.1	52.9	0.180 ± 0.011
F/ε-A/b2d	72.9	76.4 ± 0.2	75.5	64.0	66.9 ± 0.1	68.0	0.058 ± 0.001
S/ε-A/b2d	71.3	75.0 ± 0.3	74.1	63.3	66.3 ± 0.1	67.3	0.078 ± 0.002
F/IA/Cys-374	49.3	45.7 ± 0.2	53.3	50.5	48.2 ± 0.1	54.3	0.529 ± 0.003
S/IA/Cys-374	52.9	52.4 ± 0.4	56.9	53.3	53.7 ± 0.3	57.3	0.515 ± 0.004
P/IA/Cys-374	46.7	40.5 ± 0.2	50.6	49.4	46.4 ± 0.1	53.0	0.571 ± 0.008
F/IA/Cys-10	49.1	44.4 ± 0.3	53.1	51.6	50.5 ± 0.2	55.3	0.625 ± 0.009
S/IA/Cys-10	51.9	51.9 ± 0.4	55.9	52.7	53.8 ± 0.3	56.6	0.656 ± 0.015
P/IA/Cys-10	48.6	45.3 ± 0.2	52.5	50.9	50.0 ± 0.1	54.5	0.551 ± 0.008
F/Fm/Cys-74	44.0	28.6 ± 0.5	48.0	47.9	39.8 ± 0.3	51.5	0.639 ± 0.031
S/Fm/Cys-374	51.2	33.1 ± 0.8	55.4	52.6	47.1 ± 0.7	56.6	0.848 ± 0.042
F/Fm/Cys-10	50.9	49.2 ± 0.3	54.8	52.3	52.9 ± 0.2	56.1	0.584 ± 0.026
S/Fm/Cys-10	52.3	53.9 ± 0.3	56.1	52.4	54.1 ± 0.1	56.3	0.492 ± 0.018
F/NB/Lys-373	52.3	51.0 ± 0.3	56.4	52.8	51.7 ± 0.2	56.8	0.514 ± 0.038
S/NB/Lys-373	59.0	62.5 ± 0.3	63.0	58.6	61.8 ± 0.3	62.6	0.321 ± 0.026
F/5I/Cys-374	49.5	43.7 ± 0.6	53.5	49.1	42.8 ± 0.2	53.2	0.581 ± 0.008
S/5I/Cys-374	52.8	51.8 ± 0.9	56.8	53.0	52.3 ± 0.5	57.0	0.496 ± 0.014
F/5I/Cys-10	51.9	52.1 ± 0.1	55.8	52.5	53.3 ± 0.1	56.4	0.523 ± 0.007
S/5I/Cys-10	53.0	52.3 ± 0.1	56.9	52.5	53.5 ± 0.1	56.4	0.543 ± 0.004
F/DE/Gln-41	54.5	57.5 ± 0.5	58.6	54.1	53.9 ± 0.3	58.2	0.592 ± 0.008
S/DE/Gln-41	56.5	67.4 ± 0.8	60.6	56.4	58.5 ± 0.7	60.5	0.576 ± 0.009
F/FI/Lys-61	47.5	42.9 ± 0.2	51.4	48.5	44.7 ± 0.2	52.3	0.465 ± 0.010
S/FI/Lys-61	48.2	43.1 ± 0.2	52.1	50.0	46.9 ± 0.3	53.7	0.557 ± 0.012

The angles are in degrees.
The first column indicates the sample, the fluorescent dye, and the labeling site.
The last column contains the values for the number of isotropic probes in the H + I model.
The abbreviations are as listed in Table 4.
For the PAC and ZAC approximations, Φ_A and Φ_E are estimated from S_A and S_E, respectively (see Materials and Methods).
The values of the angles between absorption and emission dipoles, γ, are from Table 2 for FITC, DED, 5-IAF, TRITC-phalloidin, and 1,5-IAEDANS.
For FITC-phalloidin, NBD-Cl, fluorescein-maleimide, and ε-ADP, the values for γ are 14, 20, 31, and 32°, respectively.

ally fast compared to the fluorescence decay. Our time-resolved data indicate that these assumptions cannot be made in this system. Therefore, we abandoned the Dale et al. analysis that we initially adopted (Van Der Meer et. al., 2001), and explored the PAC and ZAC approximations and the H + I model.

Polymerization of actin is accompanied by only minor changes in the steady-state anisotropy values, which are much lower than the limiting anisotropy values. This suggests the probes have significant mobility even after polymerization (Table 2). The dye that appears most immobilized after polymerization is DED attached at the Gln-41. The current models of F-actin suggest that this particular residue is on a solvent-accessible, mobile loop of subdomain 2 and participates in the actin-actin contacts (Holmes et al., 1990; Lorenz et al., 1993; Tirion et al., 1995).

Steady-state anisotropy measurements showed a significant increase in the ratio of the steady-state anisotropy over its limiting value (r_{ss}/r_0) in both G- and F-actin upon S1 binding (Table 2). Higher values of this ratio suggest there is an increased immobilization of dyes located in different areas of the thin filament in the presence of S1. However, the decrease in probe mobilities occurred without significant alterations in the lifetimes of the probes (Table 1). This suggests that S1 binding, rather than altering the microenvironments of the dyes, restricts segmental motions within the actin molecule. The S1-induced effects had a cooperative character because saturation of the observed effects occurred at four times less than equimolar ratios of S1 (Table 3).

The binding of myosin heads changes the orientation of fluorophores attached to different sites in actin filaments (Tables 3, 4, and 5), but the directions of these rotations depend on the location of the sites. In the strong-binding rigor state, the fluorophores at the center of the filament rotate toward the filament axis, whereas the dyes at the periphery of the filament rotate away from this axis. When myosin heads bind in the weak-binding state, the reorientations are in the opposite directions, i.e., away from the axis for the dyes at the center and toward the axis for the fluorophores in the periphery.

Combined analysis of changes in the orientation of the probes using the Holmes et al. (1990) model of F-actin

suggests that fluorophores located in the small domain (subdomains 1 and 2) rotate around the monomer axis in a plane perpendicular to the filament axis (Holmes et al., 1990). Subsequently, Tirion et al. (1995) proposed a propeller-type motion of the large and small domains involving a rotation and slewing of these domains around a ''hinge'' between them (Tirion et al., 1995). Thus, the large and small domains appear to rotate, and this motion appears to increase when myosin heads bind, depending on the state of the bound nucleotide. During weak binding, S1 is predominantly attached to subdomain 1 of actin (monomer n) and therefore can exert little or no torque on the filament. However, in the strong binding state, the *N*-terminus of myosin light chain 1 also attached to subdomain 2 of monomer $n-1$. This two-point attachment could provide the structural basis for the rotation of the actin monomers demonstrated in this report.

Our data suggest that the direction of the rotation is opposite for the weak and strong binding states. These data also suggest that the above-mentioned alterations in the structure of actin monomers and filaments can be cooperatively propagated along the filament to adjacent subunits to the original S1 binding site. Orlova and Egelman (2000) recently demonstrated that actin monomers can adopt different orientations within a filament and thus the monomer may rotate relative to the filament axis.

Taken together, our data constitute a substantial and comprehensive investigation of the rotational motions of actin monomers during strong and weak binding states of S1. We show that monomers in F-actin are dynamic and that binding of a myosin head invokes a concerted structural change in its neighboring monomers that is best described in terms of differential rotation of its domains. Our findings underscore the conclusion that actin is not simply a passive structural element of the contractile apparatus.

The authors thank Drs. M. F. Morales and E. Reisler for helpful discussions, M. Khoroshev and I. Vdovina for technical assistance, A. Biktashev for writing the computer programs, and Dr M. Miki for advice regarding labeling procedures.

This research was supported by Russian Basic Research Foundation grant 01-04-49310 to Y.B., by the National Health & Medical Research Council of Australia and the Australian Research Council, and by the Kentucky NASA Experimental Program to Stimulate Competitive Research, under National Aeronautics and Space Administration grant NCC5-571. I.D. was the recipient of a Faculty of Medicine scholarship and a traveling fellowship of the Australian Academy of Science.

REFERENCES

Andreev, O. A., R. Takashi, and J. Borejdo. 1995. Fluorescence polarization study of the rigor complexes formed at different degrees of saturation of actin filaments with myosin subfragment-1. *J. Muscle Res. Cell Motil.* 16:353–367.

Borejdo, J., O. Assulin, T. Ando, and S. Putnam. 1982. Cross-bridge orientation in skeletal muscle measured by linear dichroism of an extrinsic chromophore. *J. Mol. Biol.* 158:391–414.

Borejdo, J., and S. Putnam. 1977. Polarization of fluorescence from single skinned glycerinated rabbit psoas fibres in rigor and relaxation. *Biochim. Biophys. Acta.* 459:578–595.

Borovikov, J., and S. Putnam. 1977. Polarization of fluorescence from single skinned glycerinated rabbit psoas fibres in rigor and relaxation. *Biochim. BIophys. Acta.* 459:578–595.

Borovikov, Yu. S. 1999. Conformational changes of contractile proteins and their role in muscle contraction. *Int. Rev. Cytol.* 189:267–301.

Borovikov, Yu. S., and N. B. Gusev. 1983. Effect of troponin-tropomyosin complex and Ca^{2+} on conformational changes in F-actin induced by myosin subfragment-1. *Eur. J. Biochem.* 136:363–369.

Borovikov, Yu. S., K. Y. Horiuchi, S. V. Avrova, and S. Chacko. 1996. Modulation of actin conformation and inhibition of actin filament velocity by calponin. *Biochemistry.* 35:13849–13857.

Borovikov, Yu. S., and I. Kakol. 1991. Conformational changes of contractile proteins accompanying modulation of skeletal muscle contraction. Polarized microfluorimetry investigations. *Gen. Physiol. Biophys.* 10:245–264.

Borovikov, Yu. S., and D. I. Levitsky. 1989. The effect of myosin light chain phosphorylation and Mg^{2+} on the conformation of myosin in thick filaments of glycerinated fibers of rabbit skeletal muscle. *Eur. J. Biochem.* 183:83–88.

Borovikov, Yu. S., J. Moraczewska, M. I. Khoroshev, and H. Strzelecka-Golaszewska. 2000. Proteolytic cleavage of actin within the DNase-I-binding loop changes the conformation of F-actin and its sensitivity to myosin binding. *Biochim. Biophys. Acta.* 1478:138–151.

Borovikov,Yu. S., G. N. Vinogradova, I. M. Rozanov, and I. I. Barskii. 1974. Estimation of the magnitude of depolarization induced by microobjectives during polarization fluorescence measurements. *Tsitologiya.* 16:1045–1050.

Bernhardt, R., N. T. Ngoc Dao, H. Stiel, W. Schwarze, J. Friedrich, G. R. Janig, and K. Ruckpaul. 1983. Modification of cytochrome P-450 with fluorescein isothiocyanate. *Biochim. Biophys. Acta.* 745:140–148.

Bremel, R. D., and A. Weber. 1972. Cooperation within actin filament in vertebrate skeletal muscle. *Nature.* 238:97–101.

Burghardt, T. P., A. R. Cruz-Walker, S. Park, and K. Ajtai. 2001. Conformation of myosin interdomain interactions during contraction: Deductions from muscle fibers using polarized fluorescence. *Biochemistry.* 40:4821–4833.

Chalovich, J. M., L. E. Greene, and E. Eisenberg. 1983. Crosslinked myosin subfragment 1: a stable analog of the subfragment-1- ATP complex. *Proc. Natl. Acad. Sci. USA.* 80:4909–4913.

Cooke, R. 1997. Actomyosin interaction in striated muscle. *Physiol. Rev.* 77:671–697.

Dale, R. E., S. C. Hopkins, U. A. van der Heide, T. Marszalek, M. Irving, and Y. E. Goldman. 1999. Model-independent analysis of the orientation of fluorescent probes with restricted mobility in muscle fibers. *Biophys. J.* 76:1606–1618.

Detmers, P., A. Weber, M. Elzinga, and R. E. Stephens. 1981. 7-chloro-4-nitrobenzeno-2-oxa-1,3-diazole actin as a probe for actin polymerization. *J. Biol. Chem.* 256:99–105.

dos Remedios, C. G., R. G. C. Millikan, and M. F. Morales. 1972. Polarization of tryptophan fluorescence from single striated muscle fibers. A molecular probe of contractile state. *J. Gen. Physiol.* 59:103–120.

Drewes, G., and H. Faulstich. 1991. A reversible conformational transition in muscle actin is caused by nucleotide exchange and uncovers cysteine in position 10. *J. Biol. Chem.* 266:5508–5513.

Egelman, E. H., N. Francis, and D. J. DeRosier. 1982. F-actin is a helix with a random variable twist. *Nature.* 298:131–135.

Geeves, M. A. 1991. The dynamics of actin and myosin association and the crossbridge model of muscle contraction. *Biochem. J.* 274:1–14.

Gratton, E., and M. Limkeman. 1983. A continuously variable frequency cross-correlation phase fluorometer with picosecond resolution. *Biophys. J.* 44:315–324.

Holmes, K. C., D. Popp, W. Gebhard, and W. Kabsch. 1990. Atomic model of the actin filament. *Nature*. 347:44–49.

Hudson, E. N., and G. Weber. 1973. Synthesis and characterization of two fluorescent sulfhydryl reagents. *Biochemistry*. 12:4154–4161.

Huxley, H. E., A. Stewart, H. Sosa, and T. Irving. 1994. X-ray diffraction measurements of the extensibility of actin and myosin filaments in contracting muscle. *Biophys. J*. 67:2411–2421.

Ioffe, V. A., Yu. S. Borovikov, I. I. Barskii, and Y. M. Rozanov. 1974. A two-channel polarization microfluorimeter. *Tsitologiya*. 16:112–116.

Irving, M. 1996. Steady-state polarization from cylindrically symmetric fluorophores undergoing rapid restricted motion. *Biophys. J*. 70:1830–1835.

Irving, M. A., T. St Claire, C. Sabido-David, J. S. Craik, B. Brandmeier, J. Kendrick-Jones, J. E. Corrie, D. R. Trentham, and Y. E. Goldman. 1995. Tilting of the light-chain region of myosin during step length changes and active force generation in skeletal muscle. *Nature*. 375: 688–691.

Kakol, I., Yu. S. Borovikov, D. Szczesna, V. P. Kirillina, and D. I. Levitsky. 1987. Conformational changes of F-actin in myosin-free ghost single fibre induced by either phosphorylated or dephosphorylated heavy meromyosin. *Biochim. Biophys. Acta*. 913:1–9.

Kaulin, A. B. 1968. Polarizational fluorescence of stained muscle fibers. II. Rotational depolarization of fluorescence. *Tsitologiya*. 10:184–191.

Khoroshev, M. I. and Yu. S. Borovikov. 1991. The ghost muscle fiber with thin filaments reconstructed from nonmuscle actin—a model for studying the cytoskeleton using polarization microfluorimetry. *Tsitologiya*. 33: 76–79.

Khoroshev, M. I., I. Moraczewska, H. Strzelecka-Golaszewska, and Yu. S. Borovikov. 2000. Cleavage of DNA-binding loops of actin by subtilisin prevents formation of a strong type of myosin binding with actin. *Tsitologiya*. 42:964–76.

Kim, E., C. J. Miller, M. Motoki, K. Seguro, A. Muhlrad, and E. Reisler. 1996. Myosin-induced changes in F-actin: fluorescence probing of subdomain 2 by dansyl ethylenediamine attached to Gln-41. *Biophys. J*. 70: 1439–1446.

Kishino, A., and T. Yanagida. 1988. Force measurements by micromanipulation of a single actin filament by glass needles. *Nature*. 334:74–76.

Kojima, H., A. Ishijima, and T. Yanagida. 1994. Direct measurement of stiffness of single actin filaments with and without tropomyosin by in vitro nanomanipulation. *Proc. Natl. Acad. Sci. USA*. 91:12962–12966.

Kouyama, T., and K. Mihashi. 1980. Pulse-fluorometry study on actin and heavy meromyosin using F-actin labeled with N-(1-pyrene)maleimide. *Eur. J. Biochem*. 105:279–287.

Laemmli, U. K. 1970. Cleavage of structural proteins during the assembly of the head of bacteriophage T4. *Nature*. 227:680–685.

Lorenz, M., D. Popp, and K. C. Holmes. 1993. Refinement of the F-actin model against X-ray fiber diffraction data by the use of a directed mutation algorithm. *J. Mol. Biol*. 234:826–836.

Lowry, O. H., N. J. Rosebrough, A. L. Farr, and R. J. Randall. 1951. Protein measurement with the folin-phenol reagents. *J. Biol. Chem*. 193:265–275.

Lymn, R. W., and E. W. Taylor. 1971. Mechanism of adenosine triphosphate hydrolysis by actomyosin. *Biochemistry*. 10:4617–4624.

Miki, M., C. G. dos Remedios, and J. A. Barden. 1987. Spatial relationship between the nucleotide-binding site, Lys-61 and Cys-374 in actin and a conformational change induced by myosin subfragment-1 binding. *Eur. J. Biochem*. 168:339–345.

Moens, P. D. J., D. J. Yee, and C. G. dos Remedios. 1994. Determination of the radial coordinates of Cys-374 in F-actin using fluorescence resonance energy transfer spectroscopy: effect of phalloidin on polymer assembly. *Biochemistry*. 33:13102–13108.

Morales, M. F. 1984. Calculation of the polarized fluorescence from a labeled fiber. *Proc. Natl. Acad. Sci. USA*. 81:8145–8156.

Orlova, A., and E. H. Egelman. 1997. Cooperative rigor binding of myosin to actin is a function of F-actin structure. *J. Mol. Biol*. 265:469–474.

Orlova, A., and E. H. Egelman. 2000. F-actin retains a memory of angular order. *Biophys. J*. 78:2180–2185.

Popp, D., Y. Maeda, A. A. Stewart, and K. C. Holmes. 1991. X-ray diffraction studies on muscle regulation. *Adv. Biophys*. 27:89–103.

Prochniewicz, E., and D. D. Thomas. 1997. Perturbations of functional interactions with myosin induce long-range allosteric and cooperative structural changes in actin. *Biochemistry*. 36:12845–12853.

Rayment, I., W. Rypniewski, K. Schmidt-Base, R. Smith, D. R. Tomchik, M. M. Benning, D. A. Winkelman, G. Wesenberg, and H. M. Holden. 1993. Three dimensional structure of myosin subfragmen-1: a molecular motor. *Science*. 261:50–58.

Rozanov, Y.M., N. A. Chernogriadskaya, I. Y. Barsky, Yu. S. Borovikov, and M. S. Shudel. 1971. Ultraviolet polarization fluorescence of muscle fibers and some other anisotropic cytological objects. *Tsitologiya*. 13: 190–200.

Spencer, R. D., and G. Weber. 1970. Influence of Brownian rotations and energy transfer upon measurements of fluorescence lifetimes. *J. Chem. Phys*. 52:1654–1663.

Spudich, J. A., and S. Watt. 1971. The regulation of rabbit skeletal muscle contraction. I. Biochemical studies of the interaction of the tropomyosin-troponin complex with actin and the proteolytic fragments of myosin. *J. Biol. Chem*. 246:4866–4871.

Stokes, D. L., and D. J. DeRosier. 1987. The variable twist of actin and its modulation by actin-binding proteins. *J. Cell Biol*. 104:1005–1017.

Szczesna, D., Yu. S. Borovikov, and A. Sobieszek. 1989. Interaction of tropomyosin with F-actin-heavy meromyosin complex. *Biol. Chem. Hoppe-Seyler*. 370:399–407.

Takashi, R. 1979. Fluorescence energy transfer between subfragment-1 and actin points in the rigor complex of actosubfragment-1. *Biochemistry*. 18:5164–5169.

Takashi, R., J. Duke, K. Ue, and M. F. Morales. 1976. Defining the ''fast-reacting'' thiols of myosin by reaction with 1, 5 IAEDANS. *Arch. Biochem. Biophys*. 175:279–283.

Tirion, M. M., D. ben-Avraham, M. Lorenz, and K. C. Holmes.1995. Normal modes as refinement parameters for the F-actin model. *Biophys. J*. 68:5–12.

Tregear, R., and R. A. Mendelson. 1975. Polarization from a helix of fluorophores and its relation to that obtained from muscle. *Biophys. J*. 15:455–467.

Van Der Meer, B. W., Yu. S. Borovikov, I. V. Dedova, and C. G. dos Remedios. 2001. Elastic zig-zag model of actin filaments as a framework for fluorescence depolarization: theory and relation to published approaches. *Biophys. J*. 80:75a. (Abstr.)

Wakabayashi, K., Y. Sugimoto, H. Tanaka, Y. Ueno, Y. Takezawa, and Y. Amemiya. 1994. X-ray diffraction evidence for the extensibility of actin and myosin filaments during muscle contraction. *Biophys. J*. 67: 2422–2435.

Weeds, A. G., and B. Pope. 1977. Studies on the chymotryptic digestion of myosin. Effects of divalent cations on proteolytic susceptibility. *J. Mol. Biol*. 111:129–157.

Wells, J. A., and R. G. Yount. 1979. Active site trapping of nucleotides by crosslinking two sulfhydryls in myosin subfragment 1. *Proc. Natl. Acad. Sci. USA*. 76:4966–4970.

White, H. D., and E. W. Taylor. 1976. Energetics and mechanism of actomyosin adenosine triphosphatase. *Biochemistry*. 15:5818–5826.

Wilson, M. G. A., and R. A. Mendelson. 1983. A comparison of order and orientation of cross-bridges in rigor and relaxed muscle fibres using fluorescence polarization. *J. Muscle Res. Cell Motil*. 4:671–693.

Yanagida, T., M. Nakase, K. Nishiyama, and F. Oosawa. 1984. Direct observation of motion of single F-actin filaments in the presence of myosin. *Nature*. 307:58–60.

Yanagida, T., and F. Oosawa. 1978. Polarized fluorescence from ε-ADP incorporated into F-actin in a myosin-free single fibre: conformation of F-action and changes induced in it by heavy meromyosin. *J. Mol. Biol*. 126:507–524.